Remote Sensing of Environment 114 (2010) 2219–2228

Contents lists available at ScienceDirect

Remote Sensing of Environment

journal homepage: www.elsevier.com/locate/rse

Evaluating multispectral remote sensing and spectral unmixing analysis for crop residue mapping

Anna Pacheco *, Heather McNairn

Agriculture and Agri-Food Canada, 960, Carling Avenue, Ottawa, Ontario K1A 0C6

A R T I C L E I N F O

Article history:
Received 11 December 2009
Received in revised form 21 April 2010
Accepted 25 April 2010

Keywords:
Tillage
Crop residue
Non-photosynthetic vegetation
SPOT
Landsat TM
Spectral unmixing analysis
Endmembers

A B S T R A C T

Tillage practices can affect the long term sustainability of agricultural soils as well as a variety of soil processes that impact the environment. Crop residue retention is considered a soil conservation practice given that it reduces soil losses from water and wind erosion and promotes sequestration of carbon in the soil. Spectral unmixing estimates the fractional abundances of surface targets at a sub-pixel level and this technique could be helpful in mapping and monitoring residue cover. This study evaluated the accuracy with which spectral unmixing estimated percent crop residue cover using multispectral Landsat and SPOT data. Spectral unmixing produced crop residue estimates with root mean square errors of 17.29% and 20.74%, where errors varied based on residue type. The model performed best when estimating corn and small grain residue. Errors were higher on soybean fields, due to the lower spectral contrast between soil and soybean residue. Endmember extraction is a critical step to successful unmixing. Small gains in accuracy were achieved when using the purest crop residue- and soil-specific endmembers as inputs to the spectral unmixing model. To assist with operational implementation of crop residue monitoring, a simple endmember extraction technique is described.

1. Introduction

Tillage practices affect the long term sustainability of agricultural soils as well as a variety of soil processes that impact the environment. Tillage serves a number of purposes including preparing the soil for seeding, mitigating soil compaction, controlling weeds and incorporating fertilizers into the soil. However, tilling also disintegrates soil aggregates and reduces crop residue cover on the soil. Retention of surface crop residues is an important conservation practice as these residues protect the soil from wind and water erosion. Residues incorporated into the soil by tilling decompose more quickly. Consequently all other factors being equal, soils under no-till or conservation tillage management have higher levels of organic matter and sequester more carbon. The environmental benefits along with the savings in labour and fuel costs associated with reducing or eliminating tillage have resulted in increasing implementation of these practices. Yet growing interest in the use of crop biomass and crop residues for biofuel production may counter the benefits gained in the adoption of conservation practices (Lal & Pimentel, 2007). Consequently monitoring changes in residue management in response to policy and market influences is important.

Information on tillage activities and residue cover assists in implementing policies and programs to promote beneficial management practices (BMPs), and in monitoring the success of these initiatives. Crop residue estimates are also a critical parameter in estimating soil carbon and in modeling and monitoring improvements in carbon sequestration that follow from adjustments in land management approaches. The National Agri-environmental Health Analysis and Reporting Program (NAHARP) of Agriculture and Agri-Food Canada, Canada's agri-environmental indicator initiative, require tillage information as input to 15 of the existing 29 indicators. Since 1896, much of this information has been gathered through census surveys implemented every five years. These data are collected at the farm scale but survey results are reported in aggregate. Spatial allocation of the census data to the landscape, interpretation of census survey questions, and infrequent surveying (once every 5 years) can make it difficult to capture the spatial and temporal variability in tillage management practices (Lobb et al., 2007). Other field methods such as roadside visual surveys or line-point transects (Morrison et al., 1993) are often unable to characterize the variability of crop residue cover across an agricultural field. These methods are also tedious, time consuming and prone to human judgment errors. Rapid, accurate and objective methods to measure percent crop residue cover are thus required to meet the needs of policy, programs, land management decision-makers and carbon modelers.

With access to an increasing numbers of satellites, Earth observation can play an important role in providing residue and tillage information at spatial and temporal resolutions that support monitoring and modeling at regional and watershed scales. Several remote sensing methods have been developed to quantify percent crop residue cover, including a number of approaches that rely on

* Corresponding author.
E-mail address: anna.pacheco@agr.gc.ca (A. Pacheco).

0034-4257/$ – see front matter © 2010 Published by Elsevier Inc.
doi:10.1016/j.rse.2010.04.024

spectral indices. Indices such as the Normalized Difference Index (McNairn & Protz, 1993), the Modified Soil Adjusted Crop Residue Index (Bannari et al., 2000) and the Cellulose Absorption Index (CAI) (Nagler et al., 2000) have demonstrated good correlations with ground residue measurements. However, these indices do not directly quantify residue cover and empirical models must be developed to relate percent cover to the index values. As with all empirical approaches, these models can lack robustness when applied temporally or spatially outside of the data upon which they are developed. In addition, indices such as the CAI require narrow bands in wavelengths currently unavailable on satellites with orbits and swaths needed for large area monitoring. Classification techniques such as linear spectral unmixing analysis provide an alternative to estimate percent crop residue cover (Arsenault & Bonn, 2005; Bannari et al., 2000, 2006; Pacheco et al., 2005; Roberts et al., 1993). Unlike residue indices, spectral unmixing analysis exploits the information from all available spectral bands to establish the contribution of crop residue and other land surface components (soil and vegetation) to total reflectance.

Spectral mixture analysis is based on the principal that reflectance recorded for each pixel within an image is a combination of the reflectance from all endmembers in that pixel (i.e. soil, vegetation, residue) (Adams et al., 1995; Smith et al., 1990). Spectral unmixing is a physical-based model that determines the relative contribution or abundance of each endmember, such as crop residue, to the total reflectance recorded for each pixel. The output of spectral unmixing is a series of fraction maps which indicate the proportion (0 to 1) of each endmember present in each pixel (Adams et al., 1995; Smith et al., 1990; Tompkins et al., 1997). Spectral unmixing analysis has typically been applied to derive the fraction of multiple endmembers using hyperspectral data (Boardman, 1995; García-Haro et al., 1999; Goetz et al., 1985; Martinez et al., 2006; Staenz, 1992). However, spectral unmixing analysis requires only that the number of spectral bands be one greater than the number of desired endmembers (Adams et al., 1995; Smith et al., 1990). This technique can in principal be applied to multispectral satellites if reflectance is being determined by only a limited number of endmembers, such as soil and residue.

Spectral unmixing analysis can be implemented to map residue cover over large geographic regions. If endmembers are retrieved directly from the image, spectral unmixing will be insensitive to variations in soil and residue spectra that may result from variable environmental conditions such as moisture levels in the soil or residue. In essence, given a representative pure endmember, spectral unmixing can be applied to imagery acquired at any spatial resolution, making this approach spatially scalable. The optimal spatial resolution will largely be governed by the size of the agricultural fields in the region under consideration. One constraint however is that both near infrared (NIR) and shortwave infra-red (SWIR) imaging bands are needed to characterize residue cover (Arsenault & Bonn, 2005; Bannari et al., 2000; Biard & Baret, 1997; Roberts et al., 1993) and thus residue estimation is dependent upon the availability of satellites with these critical bands. Elvidge (1990) noted that the spectral features of residue and soil are unique in the SWIR region due to the existence of a lignin and cellulose absorption for residue, which is absent for soils.

The objective of this study is to investigate the use of multispectral data and the spectral unmixing approach for estimating percent crop residue cover. To achieve this, various endmember extraction techniques are evaluated and remote sensing derived residue products are validated against ground measurements. The feasibility of operationalizing this crop residue mapping approach is also discussed.

2. Materials and methods

2.1. Study site

Crop residue information was collected over an agricultural site in the counties of Prescott and Russell, in Eastern Ontario (45° 28′ N, 74° 44′ W) (Fig. 1). Specifically, the study site area focused on a 20-km by 10-km area between the towns of Casselman and St. Isidore. The study site is located within the South Nation River watershed where topography is relatively flat. The cropping system consists mainly of corn, soybean, small grain (wheat and barley) and pasture-forage fields which is representative of agricultural production in this region of Canada. Producers use a variety of tillage implements including chisel ploughs, moldboard ploughs and disks, while others leave fields untilled. Producers may till up to three times between crop harvest in the fall and spring seeding. The combination of tillage implements, number of tillage passes, residue type and soil properties results in a wide range of residue levels across the study site from full residue cover to almost completely exposed soil. Agricultural fields used for this study were selected based on low topographic variability, homogeneity, size, residue type and soil texture. Surveyed agricultural fields were distributed over heavy clay, clay, loamy and sandy soils (Soil Landscapes of Canada Working Group, 2007).

2.2. Remote sensing and ground data

Multispectral image data were acquired over the 2007 fall and 2008 spring tillage seasons using the SPOT and Landsat satellite sensors. In total, four images (three SPOT and one Landsat) were acquired over the study site as described in Table 1.

Ground residue information was collected from selected fields near-coincident (within approximately 1–2 days) to optical image acquisitions. Surveyed fields were closely monitored to ensure no tillage activity occurred between ground and image data collection. Between 40 and 160 fields were surveyed for each acquisition, depending upon the availability of field resources (Table 1) and field tillage conditions. Ground observations were collected using an ArcPad® (ESRI) customized data entry sheet operated from a rugged mobile computer (Xplore Tablet PC) with a built-in GPS device. This approach greatly facilitated standardization and consistency in the ground data collection.

For each field, qualitative observations were collected of the tillage implement and tillage direction, residue type, residue position and direction, and residue height. In addition, percent crop residue cover for each field was measured over one sampling site using digital ground vertical photographs. A 100×75 cm quadrat was placed on the ground with its longest side positioned perpendicular to tillage direction capturing a minimum of two tillage rows. For each field, collection of quantitative data was limited to a 90 m $\times$ 90 m area in order to reduce the errors related to the variability of percent residue cover over a whole field. Five vertical photos were acquired in the 90 m $\times$ 90 m area in a cross pattern. One photo was taken in the centre of the cross with the remaining four at the appendages of the cross. The sampling sites were positioned within each field where residue conditions appeared visually homogeneous according to field visits and interpretation of previously acquired remote sensing images. The location of the sampling point at the bottom part of the cross was recorded using a Magellan GPS device (eXplorist 210) which provides positional accuracies less than or equal to 3 m.

2.3. Ground data pre-processing

To calculate percent ground residue cover, a digital grid (1×1 cm) was superimposed on the digital photographs. The number of grid intersections overlapping a piece of crop residue was visually counted and percent residue cover was calculated by summing the number of grid intersections falling on a piece of residue divided by the total number of intersections multiplied by 100. The estimates of ground residue cover from the five photos were then averaged to provide a single residue estimate per sampling site.

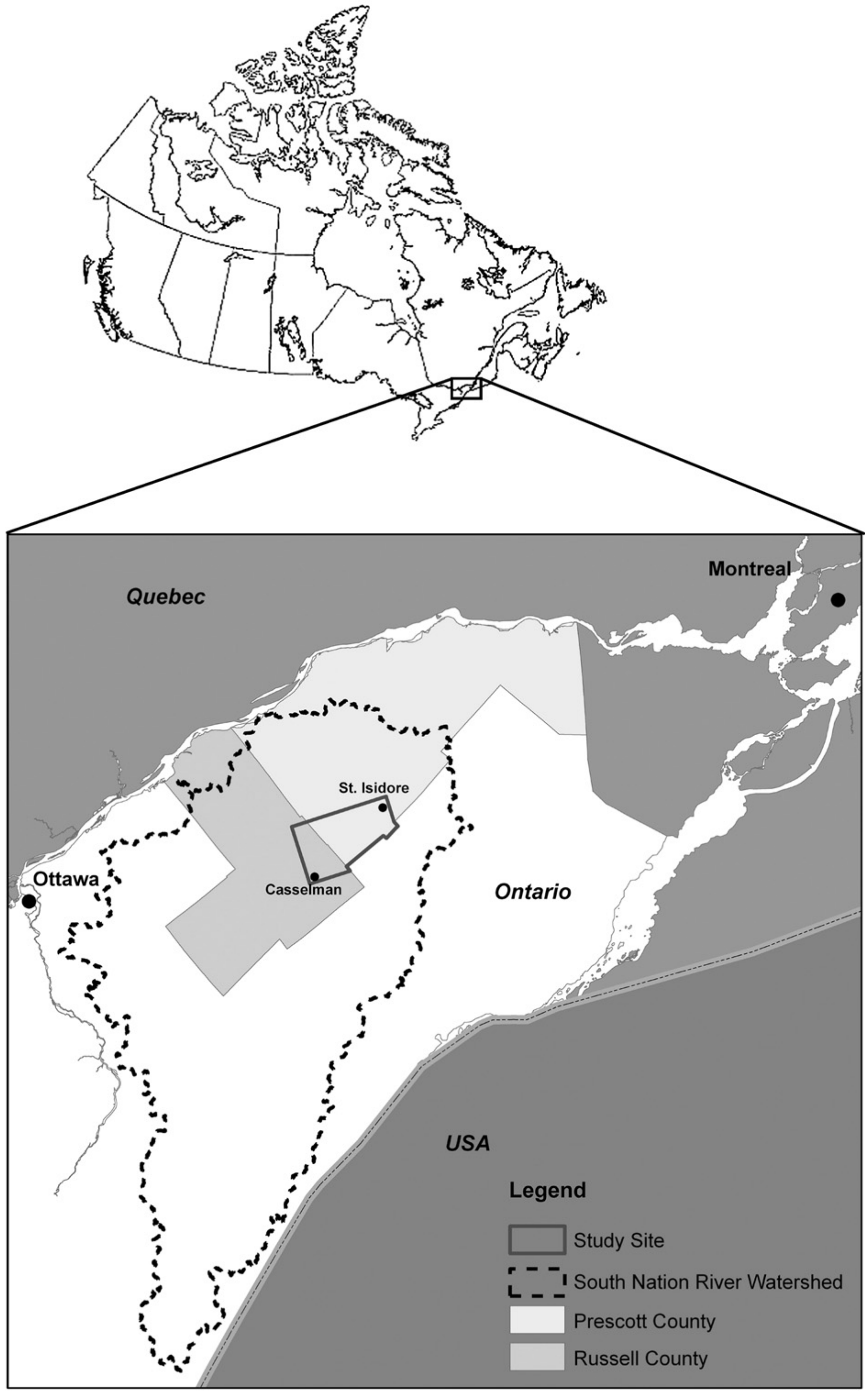

Fig. 1. Remote sensing and ground information were collected in an agricultural area of Eastern Ontario, 65 km east of Ottawa, in the counties of Prescott and Russell.

2.4. Image pre-processing

The radiance image data for SPOT and Landsat were ortho-rectified and then atmospherically corrected. The radiance image data were first ortho-rectified using the orbital information, ground control points collected from the National Road Network, Canada Level 1 (NRNC1) vector data at a scale of 1:10 000 and the Canadian Digital Elevation Data (CDED) at a scale of 1:50,000. The ortho-rectification process rendered images with one pixel accuracy or better. The images were atmospherically corrected in PCI Geomatica® software through the use of the ATCOR algorithm (Richter, 2004). ATCOR applies an atmospheric look-up table (LUT) based on a large database containing the results of radiative transfer calculations from the MODTRAN-4 radiative transfer code. The optical depth of atmospheric aerosols was calculated by comparing modeled at-sensor radiance with measured radiance in the red band of areas with dark-dense vegetation. This correction was then applied on a per-pixel basis. Image reflectance values were then used to derive residue and soil endmembers as input into the spectral unmixing model.

Table 1
Multispectral satellite images acquired over Eastern Ontario. The number of fields surveyed in total and per crop type during ground data collection is noted.

Satellite	Image date	Total fields surveyed	Small grain	Corn	Soybean
SPOT-4[a]	October 5 2007	69	13	4	52
SPOT-5[a]	November 9 2007	162	7	79	76
SPOT-4[a]	April 24 2008	140	13	81	46
Landsat-5 TM[b]	May 25 2008	39	5	28	6

[a] The SPOT-4 and -5 sensors collect image data in the following spectral range: 500–590 nm [Green], 610–680 nm [Red], 780–890 nm [NIR], and 1580–1750 nm [SWIR].
[b] Landsat-5 TM sensor collects image data in the following spectral range: 450–520 nm [Blue], 520–600 nm [Green], 630–690 nm [Red], 760–900 nm [NIR], 1550–1750 nm [SWIR], and 2080–2350 nm [SWIR].

2.5. Endmember selection

Endmember selection is the most important step to successfully unmix a reflectance data cube and produce valid fractional abundances for each pixel (Dennison & Roberts, 2003; Tompkins et al., 1997). Improper endmember selection and extraction can lead to meaningless fraction maps. Image endmembers are recognizable features in an image scene that have uniform or "pure" properties. Pure pixel endmembers are not easily retrievable at the scale of Landsat (30 m) or SPOT (20 m) imagery given the spatial resolution of these sensors (García-Haro et al., 1999; Pacheco et al., 2008). Pixels falling on agricultural land are usually a mixture of multiple materials such as vegetation (crops and weeds), soil and residue. Impure or "partially pure" endmembers cannot be utilized within spectral unmixing analysis because derived image fractions will not represent a pure material but rather a mixture of materials. Operational mapping and monitoring of residue is likely to draw upon satellites with this range of resolution and consequently, approaches must be developed to extract endmembers from this class of sensors.

Endmembers can be selected using automatic or manual extraction techniques. Automatic techniques such as principal component analysis (Smith et al., 1985), pixel purity index (Boardman, 1992) or iterative error analysis (Neville et al., 1999) eliminate the human interaction and process time, and allow the reproduction of corresponding results each time the method is used (Bateson & Curtiss, 1996; Neville et al., 1999). However, these methods assume that "pure" endmembers are contained within the image data which is not always the case (Garcia-Haro et al.). Good knowledge of the study site is crucial in selecting valid input endmembers and interpreting fraction maps. Manual endmember techniques are also a viable approach for selecting endmembers. These include endmember spectra extracted either directly from image pixels of known target materials or from spectral libraries measured in the field or extracted from the imagery. For the purpose of this study, residue and soil endmembers were selected and extracted directly from the image based on the ground data. Six different strategies for manually deriving endmembers were evaluated (Table 2). These strategies differed in their selection criteria and according to whether selected endmembers were averaged and/or adjusted for spectral impurity.

For the first five strategies, the selection of pixels to generate "pure" endmember spectra was determined by the ground data. In strategies one to four, the ground data were used to identify and average all pixels with >90% residue cover (for residue endmember spectra) and >90% soil cover (for soil endmember spectra). In the fifth approach, a single spectrum was extracted from the sampling site with the highest residue and highest soil cover based on the ground data, for each residue and soil type. Three different residues (corn, soybean and grain) and two soil types (clay and loam) were identified as endmembers for this study. Ground data collected during the various field campaigns included information on residue type whereas a soils map (scale of 1:63,360) (Soil Landscapes of Canada Working Group, 2007) was used to determine the soil type of each sampling site. Due to the similarity in spectra shape and amplitude, soil endmembers identified in the heavy clay or sandy areas were combined with the clay and loam endmembers, respectively. Some of these spectra were pure having 100% residue or 100% soil cover, while others were only partially pure (>90% residue or soil cover). Availability of pure crop residue and soil endmembers varied temporally. Pure residue endmembers were more prevalent immediately following harvest prior to significant tillage activity whereas pure soil endmembers were easier to locate near the end of tillage season once producers had prepared the seeding beds.

If pure endmembers were unavailable, pixels with the highest (>90%) residue and soil cover were identified from the ground data. These partially pure residue and soil endmembers were adjusted for their impurity by correcting their reflectance response for each spectral band. With this adjustment technique, reflectance is assumed to be linearly related to percent residue cover. Arsenault and Bonn (2005) and Sohn et al. (1999) discuss how overall reflectance of a target can be lower or higher than the average reflectance values over the entire electromagnetic spectrum, but essentially the reflectance

Table 2
Summary of endmember extraction approaches evaluated in this study.

Endmember approach	Endmember selection criteria	Adjust spectra	Endmember averaging	Number of endmember spectra
1. RES AVG–SOIL AVG	All fields with >90% residue or >90% soil as determined from ground data	Yes	Residue — All residue spectra averaged Soil — All soil spectra averaged	One residue spectra One soil spectra
2. RES SPEC–SOIL SPEC	All fields with >90% residue or >90% soil as determined from ground data	Yes	Residue — All spectra averaged within each residue type Soil — All spectra averaged within each soil type	Two residue spectra (one for corn/grain, one for soybean); Two soil spectra (one for clay, one for loam)
3. RES SPEC–SOIL AVG	All fields with >90% residue or >90% soil as determined from ground data	Yes	Residue — All spectra averaged within each residue type Soil — All soil spectra averaged	Two residue spectra (one for corn/grain, one for soybean); One soil spectra
4. RES AVG–SOIL SPEC	All fields with >90% residue or >90% soil as determined from ground data	Yes	Residue — All residue spectra averaged Soil — All spectra averaged within each soil type	One residue spectra; Two soil spectra (one for clay, one for loam)
5. RES MAX–SOIL MAX	Select spectra of field with highest residue and highest soil cover as determined from ground data	Yes	None	Two residue spectra (one for corn/grain, one for soybean); Two soil spectra (one for clay, one for loam)
6. IMG RES MAX–IMG SOIL MAX	Plot spectra of all fields with >90% residue and >90% soil cover. Select highest (residue) and (soil) spectra.	No	None	Two residue spectra (one for corn/grain, one for soybean); Two soil spectra (one for clay, one for loam)

pattern of a particular target remains a linearly scaled version of the mean overall reflectance pattern. An evaluation of this adjustment technique was done where residue fractions were tested using unadjusted and adjusted endmember spectra and validated separately. Accuracies were consistently higher by 2–3% when using the adjusted endmembers as input to the unmixing model.

The endmembers were sequentially adjusted starting with the residue endmember, followed by the soil endmember. To accomplish this, a residue reflectance adjustment (RR_{Adj}) was calculated according to:

$$RR_{Adj} = \left(\frac{RR_{pp} - SR_{pp}}{FCR_{pp} - FCS_{pp}}\right) / 100 \quad (1)$$

where RR_{pp} is the reflectance of the partially pure residue endmember, SR_{pp} the reflectance of the partially pure soil endmember, and FCR_{pp} and FCS_{pp} are the fractional residue and soil cover associated with these partially pure endmembers. The RR_{Adj} represents the reflectance per fraction of residue, and is then applied to the partially pure residue reflectance by using the following equation:

$$RR = RR_{pp} + \left(RR_{Adj} * \left(100 - FCR_{pp}\right)\right) \quad (2)$$

where RR is the residue reflectance for a pure residue endmember. This adjustment increases the partially pure residue reflectance to a reflectance that might be expected from 100% residue cover.

The reflectance of the pure residue endmember is then used to adjust the reflectance for each band of the partially pure soil endmember:

$$SR_{Adj} = \left(\frac{RR - SR_{pp}}{FCR - FCS_{pp}}\right) / 100 \quad (3)$$

where FCR is the fraction cover of a pure residue. The soil reflectance for a pure soil endmember (SR) is then calculated as follows:

$$SR = SR_{pp} - \left(SR_{Adj} * FCS_{pp}\right). \quad (4)$$

Approximately 10% of the agricultural land in Eastern Ontario is under small grain production. Small grain fields are usually harvested in August and the majority of these fields are under seeded with forage. During the fall or spring tillage season, small grain fields have either partial or full green vegetation cover, or contain dry forage vegetation. This situation results in a complex mixture of signatures that are temporally dynamic, making the identification of "pure" small grain endmembers challenging. Thus, corn residue endmembers were used to unmix small grain fields given that both residues produce similarly bright reflectances.

Residue reflectance varies depending on the type and condition of the residue, as well as the water content in the residue. Soil reflectance is largely influenced by texture, organic matter and moisture. Endmembers must be selected for input into spectral unmixing analysis in such a way that these endmembers capture the variability associated with residue and soil conditions and adequately reflect the conditions present across the site. All approaches began with the identification of specific pure endmembers for each residue type (corn and soybean) and for each of the two dominant soil textures (clay and loam). Previous research studies investigating spectral unmixing analysis (Arsenault & Bonn, 2005; South et al., 2004) have averaged input endmembers and thus in the present study, some strategies adopted a similar averaging approach (Table 2). In this approach, specific endmembers for both residue types (corn and soybean) were averaged to provide a single residue endmember (RES AVG). All soil endmembers (clay and loam) were also averaged producing a single soil endmember (SOIL AVG). Endmember averaging was meant to represent typical residue and soil conditions present across the study site.

If the spectra for different residue and soil types across the study site are too variable, a single residue or soil spectra will not adequately represent this diversity. Under these circumstances, a residue specific (RES SPEC) and/or soil-specific (SOIL SPEC) spectra is more appropriate. This study thus also explored unmixing the image datasets using two specific residue (corn and soybean) as well as two specific soil (clay and loam) endmember spectra. The two residue and two soil-specific endmembers provided four different pairings of endmember combinations (i.e. corn residue-clay soil; corn residue-loam soil; soybean residue-clay soil; soybean residue-loam soil). Unmixing was run for each endmember combination and validated based on the residue and soil type identified for each sampling plot as per the ground data and soil map (Soil Landscapes of Canada Working Group, 2007), respectively. The pairing of average endmembers with specific endmembers was also evaluated (Table 2). In these scenarios, residue specific endmembers are used in combination with soil average endmembers (RES SPEC–SOIL AVG), or conversely average residue endmembers were used with soil-specific endmembers (RES AVG–SOIL SPEC).

Successful unmixing of residue and soil contributions to total reflectance, using a few broad spectral bands, is dependent upon good contrast in spectral response between these two cover types (Biard & Baret, 1997; McNairn & Protz, 1993; Thoma et al., 2004; van Deventer et al., 1997). The endmember spectra selected must be representative but must also maintain a sufficient spectral difference between residue and soil. In the fifth approach, the ground data were used to select the field with the highest residue and soil coverage (RES MAX–SOIL MAX) for each specific residue and soil type. If the residue and soil cover were below 100% as per the ground data, then these endmembers were adjusted for their impurity according to the previously discussed adjustment approach.

Selection of pure endmembers based on quantitative ground data is time consuming due to the effort required to collect and process the ground data. Consequently, a simplification of this approach was assessed to facilitate future operational implementation. In this sixth and final approach, the selection of "pure" residue and soil endmembers was driven by the spectra extracted from the imagery (IMG RES MAX–IMG SOIL MAX), where minimal knowledge of residue and soil coverage is required. To accomplish this, all the spectra were plotted for fields with high residue and soil cover (>90%). The spectra with the highest and lowest reflectance in the NIR and SWIR spectral regions were selected for each residue and soil type endmember, respectively. By selecting endmembers based on their image reflectance response as opposed to the ground vertical photos, the requirement for quantitative ground residue data can be relaxed if not eliminated completely. Collection of more qualitative categorical ground data would be all that is required. Less labour-intensive roadside surveys could be used to identify a sample of fields with maximum (90–100%) residue and soil cover. Due to the changing nature of the environmental and atmospheric conditions of each satellite image dataset, it is recommended to extract image-specific endmembers for every image being unmixed (Bateson & Curtiss, 1996; García-Haro et al., 1999; Martinez et al., 2006; Pacheco et al., 2005).

2.6. Spectral unmixing analysis

Spectral unmixing analysis is a classification approach first developed for hyperspectral remote sensing and used to extract information from hundreds of spectral bands at a time. The fundamental assumption of linear spectral unmixing analysis is that each pixel on the surface is a physical mixture of several constituents weighted by surface abundance, and the spectrum of the mixture is a linear combination of the endmember reflectance spectra (Boardman, 1995). Within the context of this study, spectral unmixing analysis can determine the contribution of each material (or endmember) such as vegetation, soil or residue for each image pixel. Linear constrained spectral unmixing analysis is expressed with the following equation:

$$SMA \equiv R_b \equiv \sum_{i=1}^{m} f_i r_{bi} + e_b, \quad \text{in which} \sum_{i=1}^{m} f_i = 1.0, \tag{5}$$

where R_b is pixel reflectance in band b, f_i is the fractional abundance of endmember i, m is the total number of endmembers, r_{bi} is the reflectance in band b of endmember i, and e_b is the residual error in band b of the model. Constrained unmixing assumes that the sum of the fractions is one and that each fraction is greater than or equal to zero (Bateson & Curtiss, 1996; Boardman, 1995; Dennison & Roberts, 2003).

Spectral unmixing analysis can also be applied on any multispectral dataset. The only condition is that the number of derived fractions (or endmember (m) inputs) is equal to or less than the number of bands (n) of the sensor plus one ($m = n + 1$). To derive percent crop residue cover from image reflectance data, constrained linear SMA was computed using the SPUNMIX algorithm (Shepherd, 2005) in the PCI Geomatica® software. Crop residue fractions were derived and incorporated in a GIS for spatial and statistical analysis.

2.7. Validating residue fractions

To validate percent residue cover estimated by spectral unmixing analysis, ground measurements and image estimated values were compared using the coefficient of determination (R^2) and errors of estimate were quantified using the root mean square error (RMSE) statistic. RMSE was calculated with the following equation (Willmott, 1982):

$$RMSE = \sqrt{\frac{\sum_{i=1}^{n} (P_i - O_i)^2}{n}}, \tag{6}$$

where P_i is the predicted value at sample i, O_i is the observed value at sample i and n is the number of values. The RMSE indicates the magnitude of the average error produced by a model. This error is reported in the same units as the observed and predicted values. Scatterplots displaying observed and predicted variables were also generated to help evaluate and analyze the relationship between the variables (Willmott, 1982).

The relationships between observed and predicted values were also analyzed using a linear regression model. Correlations were computed based on datasets (i.e. per image date) and residue type. Then, dataset results were pooled according to residue type. Various statistics were computed for the ground residue measurements (observed values) including means and standard deviations.

3. Results

3.1. Selecting an appropriate endmember extraction approach

As described in Section 3.3, six different endmember extraction approaches were investigated as summarized in Table 2. The November 9 dataset was used to test the various endmember approaches given that it was the largest dataset available with the greatest ground data distribution. R^2 and RMSE results are illustrated in Fig. 2a and b, respectively. Overall, the difference in R^2 among the various endmember approaches was not large and did not considerably affect the correlation between measured and estimated residue cover. The greatest variability was observed for the soybean residue fields. The soybean residue spectral curve is closer in amplitude to the

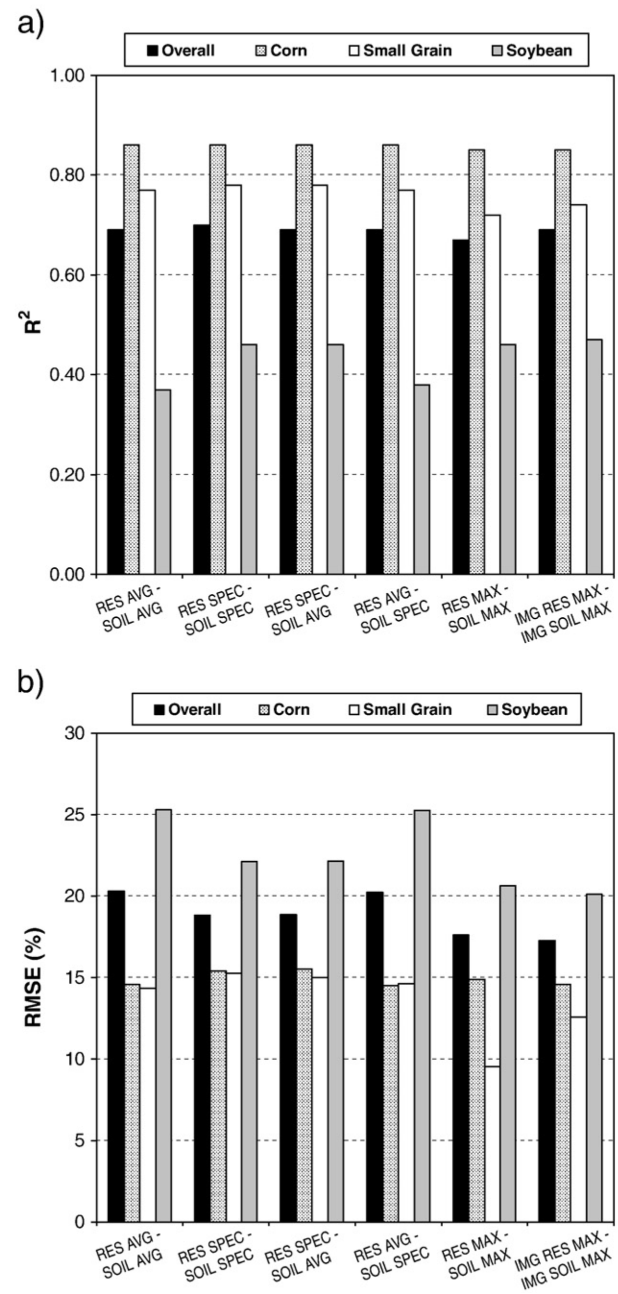

Fig. 2. Coefficient of determination (R^2) (a) and Root Mean Square Error (RMSE) (b) spectral unmixing results for the November 9th dataset derived for each endmember extraction approach.

soil spectral curve. Consequently even a minor change in either the soybean residue or soil endmember spectra can generate confusion between these two endmembers. Although statistically significant, estimated and measured percent soybean residue were only weakly correlated with R^2 values around 0.40 regardless of the endmember approach utilized. Corn residues tend to be highly reflective in both the NIR and SWIR bands. Consequently, corn residue endmembers are usually characterized by fairly high amplitude in these spectral bands and are more highly contrasted to the lower soil spectra. However when corn and soybean residue spectra are averaged, the average residue spectra is considerably higher relative to the soybean spectra and the unmixing model can mistakenly interpret these less bright soybean residues as soil.

The different endmember combinations had a greater impact on the RMSE statistics. Errors were consistently lower when individual endmembers for each residue type were used. The use of clay and loam soil-specific endmembers in the spectral unmixing model resulted in smaller gains in accuracies. This suggests that the spectral difference among crop residue types was greater than the difference between the two soil types. Spectral unmixing is best achieved when endmembers with maximum residue and soil cover were selected (based on the ground data) in comparison to results using average residue and/or average soil spectra. Using specific endmembers, the spectral amplitude difference is maximized between each residue and soil type, permitting a more distinctive definition of each endmember type and improved estimation of percent crop residue cover. When comparing crop residue fractions derived from the RES MAX–SOIL MAX and IMG RES MAX–IMG SOIL MAX approaches, results were not significantly different. RMSE does not vary more than 4% between these two endmember selection approaches. However, the latter approach would be easier to implement for large area operational monitoring given its less demanding requirement for quantitative residue ground data. Consequently, assessment of the remaining image datasets was completed using the IMG RES MAX–IMG SOIL MAX endmember approach.

3.2. Extracting residue and soil endmembers

Fig. 3a and b illustrates the endmember reflectance spectra for the corn and soybean residues, and the loam and clay soils for the 2007 and 2008 datasets, respectively. Endmember spectra were consistent with previous spectral unmixing analysis studies conducted over the same study site (Pacheco et al., 2005, 2007). As expected, crop residue spectra had higher reflectance when compared to the soil spectra. The contrast between residue and soil spectra was particularly evident in the NIR and SWIR bands. Selecting the maximum crop residue and soil spectra emphasizes this contrast, facilitating discrimination between these two cover types.

Assuming accurate radiometric and atmospheric corrections of the remote sensing imagery, environmental conditions such as weathering and moisture can significantly alter the amplitude of image spectra (Daughtry & Hunt, 2008). Endmember spectra extracted from the November 9 dataset were consistently lower than the ones from the October 5 dataset, particularly for crop residues. Typically, the spectra of crop residues are brighter shortly after harvest and their reflectance decreases (such as corn) or increases (such as soybean) as the residue undergoes weathering and decomposition, particularly after the winter season (Biard & Baret, 1997; Nagler et al., 2000; Thoma et al., 2004). In addition, climate data acquired from the Russell Weather Station (45° 15.6′ N, 75° 21.6′ W) recorded 6.8 mm of rain in the five days prior to the November 9 acquisition. No precipitation was recorded within the same time frame for the October 5 acquisition. Crop residue reflectance values decreased approximately 15% and 8%, from the October dataset to the November dataset in the SWIR and NIR bands, respectively. For the 2008 dataset, 4.4 mm of rain was recorded five days preceding the April 24 acquisition compared to 1.6 mm for the May 25 acquisition. The variations in the amplitude of the endmember spectra, resulting in changes in residue and soil moisture, indicate that endmember spectra extracted from one dataset are not transferable to another. This limitation was confirmed in preliminary analysis (Pacheco et al., 2005), implying that soil and residue endmembers are best extracted for each new image acquisition to avoid the processes and factors influencing the data (Bateson & Curtiss, 1996; García-Haro et al., 1999; Martinez et al., 2006) or different moisture conditions.

Reflectance of residue endmembers varies from one crop to the other. Overall, corn residue endmembers have the brightest reflectance, especially in the SWIR where reflectance can reach values of 70%. Residue and soil endmember variability is greater in the NIR and SWIR bands suggesting that these bands are essential for residue discrimination. Differences of reflectance in the visible bands were minimal, providing little discrimination between residue and soil. Soybean residue endmembers had the lowest reflectance of all crop residue endmembers. Soil endmembers typically reached reflectance values close to 15–25% in the NIR and 20–40% in the SWIR. The effect of weathering on the residue spectra was not observed for the 2008 dataset. Although residue endmembers selected for input varied from one dataset to the other, the residue endmember selection process proposed in this study is sufficiently robust to account for these slight variations. The spectral signatures for loam and clay soils varied slightly (Biard & Baret, 1997), likely due to organic matter and moisture retention characteristics associated with these soil textures.

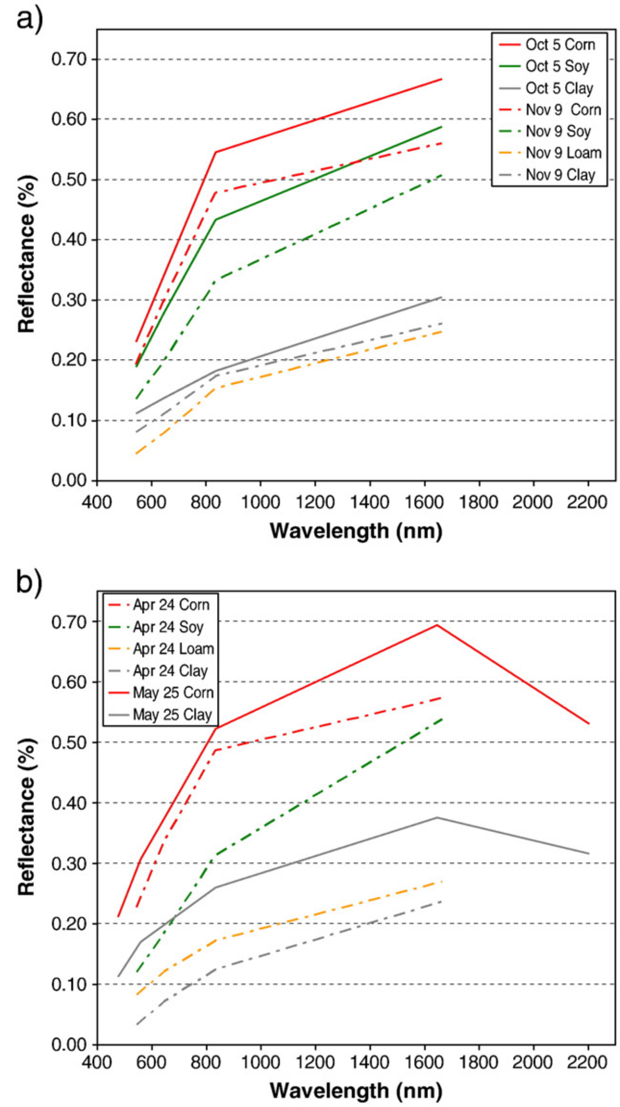

Fig. 3. Residue and soil endmember spectra for the 2007 fall (a) and 2008 spring (b) datasets. All spectra were acquired with SPOT data except for the May 25 dataset. The May 25 dataset was acquired by Landsat resulting in the difference of the spectral curves for this dataset.

3.3. Validating crop residue fractions

Crop residue fractions estimated from spectral unmixing analysis were validated against the ground data collected coincident to the image acquisitions (Table 1) using R^2 and RMSE statistics. The relationships between the image and ground residue cover are plotted for each dataset in Fig. 4 and summarized in Table 3. The crop residue cover estimated from the spectral unmixing approach was positively correlated with the ground residue data for all datasets with R^2 values

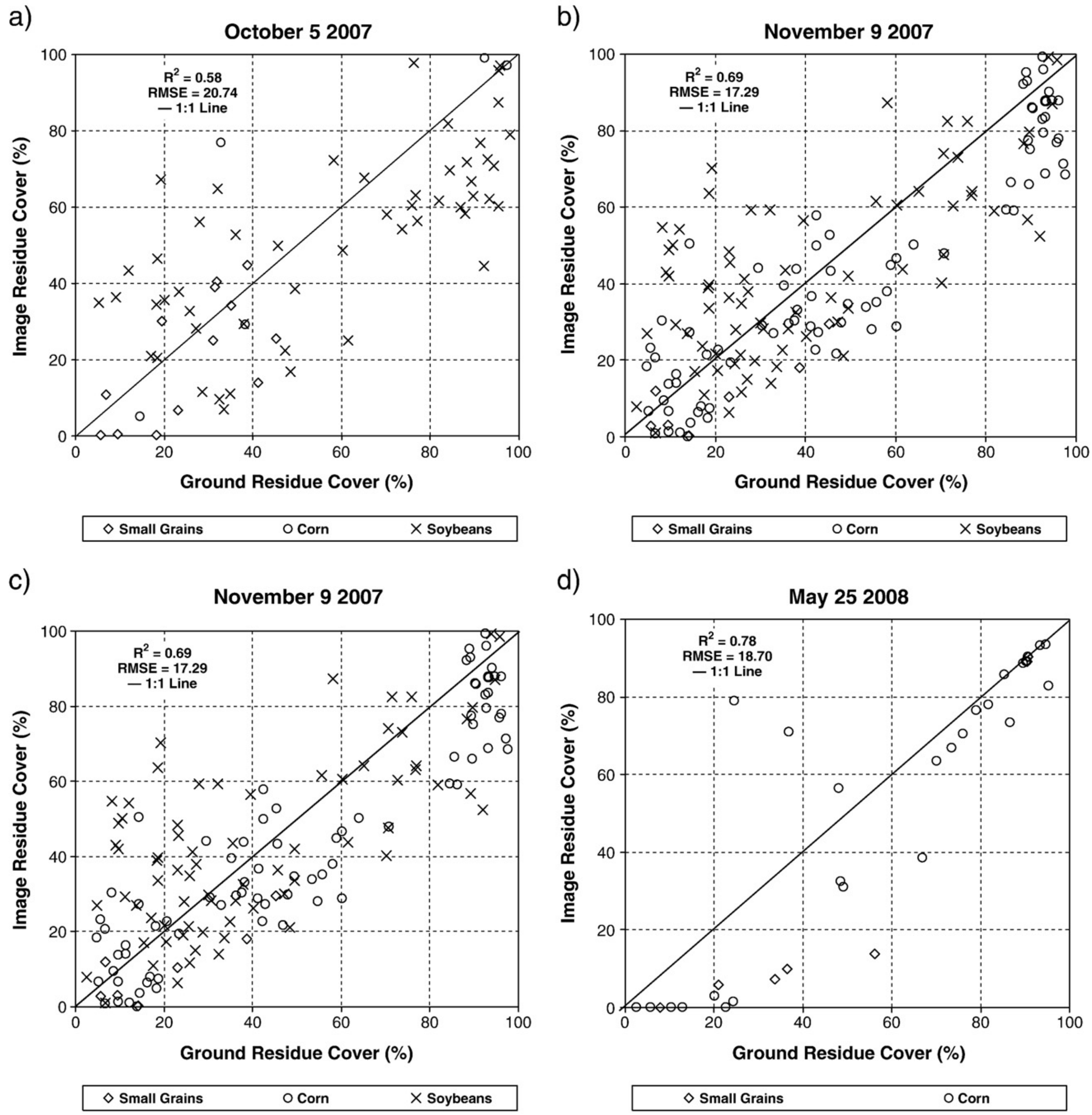

Fig. 4. Scatter plots of image residue cover vs ground residue cover using the IMG RES MAX – IMG SOIL MAX endmember combination for the October 5 2007 (a), November 9 2007 (b), April 24 2008 (c) and May 25 2008 (d) datasets.

between 0.58 and 0.78. The distribution of the ground data for the April 24 and May 25 datasets resulted in slightly higher R^2 (0.75 and 0.78, respectively). The bulk of the fields surveyed for these datasets were either under conventional tillage or no-till resulting in clusters of data. Given the cropping system prevalent in Eastern Ontario, few fields under conservation tillage (i.e. 30–60% residue cover) were present. Finding fields that fit this criterion was particularly challenging for the spring 2008 field data collection. For all datasets,

Table 3
Derived statistics from the validation of the image percent crop residue cover against the ground percent residue cover for the 2007 and 2008 datasets using the IMG RES MAX – IMG SOIL MAX endmember combination.

Dataset	All residue types		Corn		Small grain		Soybean		Corn and small grain	
	R^2	RMSE	R^2	RMSE	R^2	RMSE	R^2	RMSE	R^2	RMSE
October 5	0.58	20.74	–	–	0.45	12.91	0.49	22.28	0.86	11.52
November 9	0.69	17.29	0.85	14.60	0.74	12.58	0.47	20.11	0.85	14.44
April 24	0.75	18.48	0.81	18.15	0.59	21.42	0.67	14.17	0.79	18.67
May 25	0.78	18.70	0.98	10.92	–	–	–	–	0.78	18.70
Pooled Datasets	0.69	18.46	0.80	16.67	0.43	18.39	0.54	20.29	0.79	16.97

RMSE varied from 17.29% and 20.74% with the November 9 dataset producing the lowest errors. The spectral contrast between endmember pairs was slightly greater for all other datasets than the November 9 dataset, which suggests that the size and distribution of the sample population for the November dataset had a positive impact in the validation of the spectral unmixing model. A percent residue cover map of the November 9 2007 dataset was generated (Fig. 5).

3.4. Estimating residue cover on a crop type basis

Detecting residue cover is dependent not only on the soil texture but also on the residue type. Crop residues have different colors, textures and absorb water differently. Weathering also materializes at different rates for each type of residue. Section 3.2 illustrated how amplitudes vary from one residue type to another whereas the shape of the residue spectra remains consistent. Because of this, success at detecting percent cover of different residues will also vary, contrary to conclusions presented by Arsenault and Bonn (2005). Validation of corn residue cover was by far the most successful with R^2 greater than 0.80 and RMSEs typically around 13.00%, except for the April 24 dataset. Precipitation previous to this acquisition decreased the brightness of the corn residue and subsequently its reflectance, causing the percent residue cover to be underestimated. Thoma et al. (2004) also found that the Crop Residue Index Multiband (CRIM) performed better on corn relative to bean residues.

Validation of small grain fields revealed a greater range of R^2 (0.45 to 0.74) and RMSE values (12.58 to 21.42%). Given that the sample population was much smaller than the corn and soybean datasets, each data point has greater influence on the statistics and thus results were less robust. It must be noted as well that corn endmembers were used as input to the small grain residue spectral unmixing model because of the unavailability of "pure" small grain endmembers. Thus, this might also have contributed to the high variability in the results. Given that small grain production represents such a small portion of the cropland in Eastern Ontario (about 10%), the difficulty in extracting small grain endmembers within this cropping system will most likely be an ongoing challenge. However, these results suggest that corn residue endmembers could be used to map small grain residue cover and still achieve reasonable accuracies.

Soybean residue cover was more difficult to estimate with RMSE approximating 20.00%. The small difference in amplitude between the soil and soybean residue endmembers generates some confusion in distinguishing these surfaces from one another. In accordance with Biard and Baret (1997), the reduced contrast between the soybean residue and soil decreased the ability to detect percent residue cover. The higher overall RMSE errors are largely driven by the greater uncertainty in estimating soybean residue. Errors are reduced (by almost 2%) when pooling data from the corn and small grain fields exclusively, with errors of 11.52% and 14.44% for the October 5 and November 9 datasets respectively. For the April 24 dataset, the

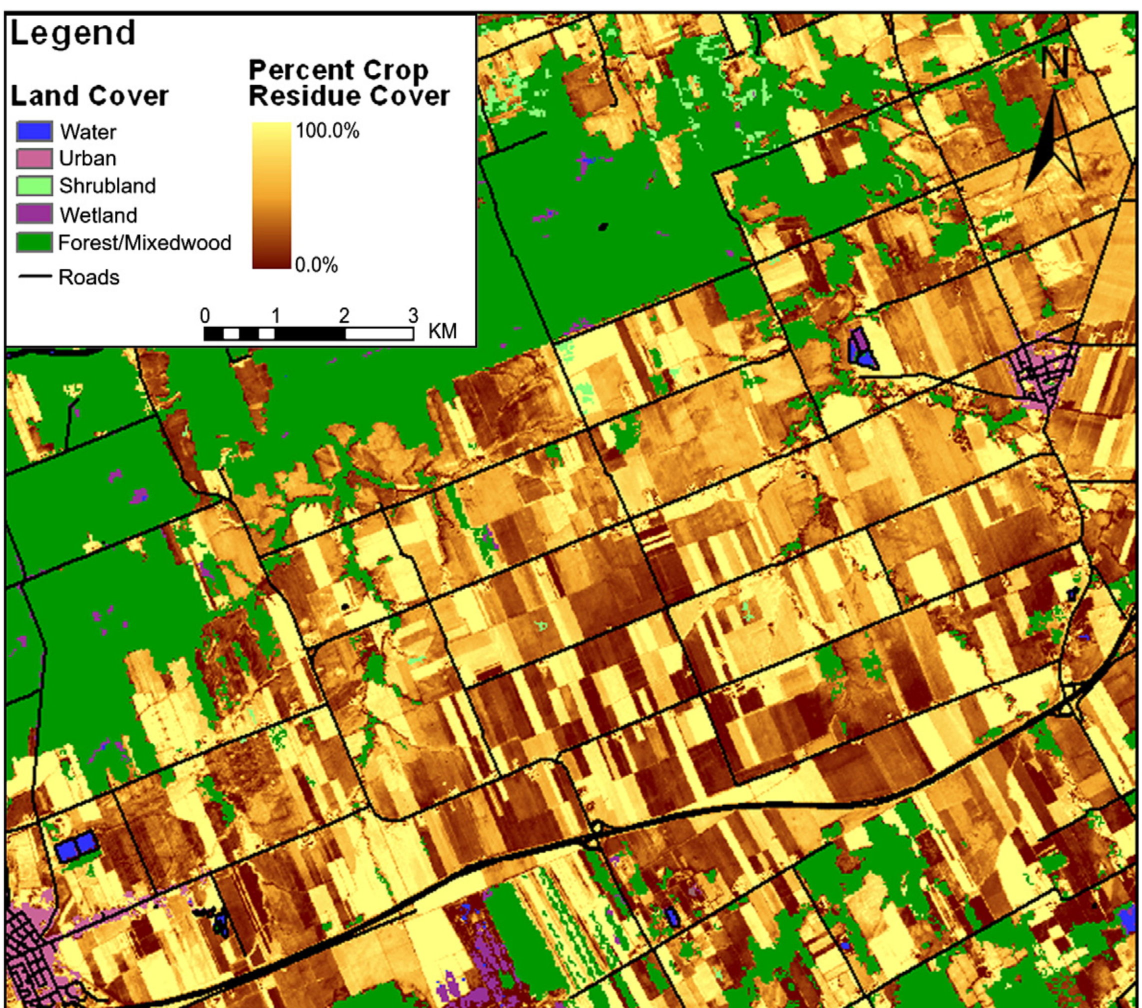

Fig. 5. Percent crop residue cover map over the Casselman/St. Isidore study site derived from spectral mixture analysis on a SPOT image acquired on November 9 2007. A land cover mask (non agricultural areas) is overlaid on the residue cover map.

soybean error was low at 14.17% and pooling the corn and small grain fields did not achieve the same reductions in error given that the small grain RMSE was unusually high.

4. Conclusions

Results from this study demonstrated that spectral unmixing analysis applied to multispectral data, more specifically Landsat and SPOT imagery, can produce crop residue estimates with root mean square errors between 17.29% and 20.74%. Errors were higher for soybean residues. This was expected given the reduced difference in the amplitude of the spectra between soybean residue and its soil background. Exploration of various endmember approaches found that although results did not vary greatly, it was possible to improve accuracies using a crop specific residue endmember. These endmembers were chosen using ground data collected at the time of image acquisition. Individual residue endmembers (corn and soybean) had higher reflectance; the soil endmembers (clay and loam) had lower reflectance. Inputs of individual endmembers to the spectral unmixing analysis produced superior results relative to the use of a single average residue endmember or soil endmember. However, this approach still represents some challenges if crop residue monitoring were to be implemented operationally. The final endmember approach consisted of extracting high-reflectance crop residue and low-reflectance soil endmembers directly from the imagery, using more qualitative knowledge of field residue levels. This approach demonstrated similarly positive results to the other endmember selection approaches. However this approach does not depend upon large volumes of quantitative data, making its implementation less resource-intensive and timelier.

Acknowledgements

Many others contributed to the completion of this research study. The authors would like to acknowledge Eric Gauthier, Amine Merzouki, Jiali Shang, Catherine Champagne, Pierre-Yves Gasser, Patrick Rollin, Leander Campbell, Nicolas Svacina and Christopher Roth for their assistance in field data collection. Remote sensing and ground data processing was carried out with the help of Graham Pope and Francis Langelier. This research was partly funded by the Canadian Space Agency under the Government Related Initiatives Program (GRIP) and supported by the National Land and Water Information Service (AAFC).

References

Adams, J. B., Sabol, D. E., Kapos, V., Filho, R. A., Roberts, D. A., Smith, M. O., et al. (1995). Classification of multispectral images based on fractions of endmembers: Application to land-cover change in the Brazilian Amazon. *Remote Sensing of Environment*, *52*, 137−154.

Arsenault, E., & Bonn, F. (2005). Evaluation of soil erosion protective cover by crop residues using vegetation indices and spectral mixture analysis of multispectral and hyperspectral data. *Catena*, *62*, 157−172.

Bannari, A., Haboudane, D., & Bonn, F. (2000). Intérêt du moyen infrarouge pour la cartographie des résidus de cultures. *Canadian Journal of Remote Sensing*, *26*(5), 384−393.

Bannari, A., Pacheco, A., Staenz, K., McNairn, H., & Omari, K. (2006). Estimating and mapping crop residues cover on agricultural lands using hyperspectral and IKONOS data. *Remote Sensing of Environment*, *104*, 447−459.

Bateson, A., & Curtiss, B. (1996). A method for manual endmember selection and spectral unmixing. *Remote Sensing of Environment*, *55*, 229−243.

Biard, F., & Baret, F. (1997). Crop residue estimation using multiband reflectance. *Remote Sensing of Environment*, *59*, 530−536.

Boardman, J. W. (1992). Automating spectral unmixing of AVIRIS data using convex geometry. In R. O. Green (Ed.), *Summaries of the 4th Airborne Geoscience ConferenceJPL Publication 93-26*, *Vol. 1*. (pp. 11−14) Pasadena, California, USA: Jet Propulsion Laboratory.

Boardman, J. W. (1995). Analysis, understanding and vizualization of hyperspectral data convex sets in N-Space. *Proceedings of SPIE's International Conference on Imaging Spectrometry*, *2480*. (pp. 14−20) Orlando, Florida.

Daughtry, C. S. T., & Hunt, E. R. J., Jr. (2008). Mitigating the effects of soil and residue water contents on remotely sensed estimates of crop residue cover. *Remote Sensing of Environment*, *112*, 1647−1657.

Dennison, P. E., & Roberts, D. A. (2003). The effects of vegetation phenology on endmember selection and species mapping in Southern California Chaparral. *Remote Sensing of Environment*, *87*, 295−309.

Elvidge, C. D. (1990). Visible and near infrared reflectance characteristics of dry plant materials. *International Journal of Remote Sensing*, *11*(10), 1775−1795.

García-Haro, F. J., Gilabert, M. A., & Meliá, J. (1999). Extraction of endmembers from spectral mixtures. *Remote Sensing of Environment*, *68*, 237−253.

Goetz, A. F. H., Vane, G., Solomon, J. E., & Rock, B. N. (1985). Imaging spectrometry for earth remote sensing. *Science*, *228*(4704), 1147−1153.

Lal, R., & Pimentel, D. (2007). Biofuels from crop residues. *Soil and Tillage Research*, *93*, 237−238.

Lobb, D. A., Huffman, E., & Reicosky, C. (2007). Importance of information on tillage practices in the modeling of environmental processes and in the use of environmental indicators. *Journal of Environmental Management*, *82*, 377−387.

Martinez, P. J., Perez, R. M., Plaza, A., Aguilar, P. L., Cantero, M. C., & Plaza, J. (2006). Endmember extraction algorithms from hyperspectral images. *Annals of Geophysics*, *49*(1), 93−101.

McNairn, H., & Protz, R. (1993). Mapping corn residue cover on agricultural fields in Oxford County, Ontario, using thematic mapper. *Canadian Journal of Remote Sensing*, *19*(2), 152−159.

Morrison, J. E., Jr, Huang, C., Lightle, D. T., & Daughtry, C. S. T. (1993). Residue measurement techniques. *Journal of Soil and Water Conservation*, *48*, 479−483.

Nagler, P. L., Daughtry, C. S. T., & Goward, S. N. (2000). Plant litter and soil reflectance. *Remote Sensing of Environment*, *71*, 207−215.

Neville, R. A., Staenz, K., Szeredi, T., Lefebvre, J., & Hauff, P. (1999). Automatic endmember extraction from hyperspectral data for mineral exploration. In *Proceedings of Fourth International Airborne Remote Sensing Conference and Exhibition / 21st Canadian Symposium on Remote Sensing*, *vol. 2*. (pp. 891−897) Ottawa, Canada.

Pacheco, A., Bannari, A., Staenz, K., & McNairn, H. (2008). Deriving percent crop cover over agriculture canopies using hyperspectral remote sensing. *Canadian Journal of Remote Sensing*, *34*, 110−123.

Pacheco, A., McNairn, H., Gauthier, E., & Holmstrom, D. (2007). Using earth observation to monitor no-till practices over agricultural crops in Eastern Ontario and Prince Edward Island, Canada. *CRSS/ASPRS 2007 Specialty Conference, Ottawa, Ontario, Canada, October 28 – November 1*.

Pacheco, A., McNairn, H., & Smith, A. M. (2005). Multispectral indices and advances classification techniques to detect percent residue cover over agricultural crops using Landsat data. *SPIE Optics and Photonics Proceedings, San Diego, California, USA, August 13–17*.

Richter, R. (2004). *Atmospheric/Topographic Correction for Satellite Imagery: Atcor 2/3 Users Guide Version 6.0.*Wessling, Germany: DLR German Aerospace Centre 71 pages.

Roberts, D. A., Smith, M. O., & Adams, J. B. (1993). Green vegetation, nonphotosynthetic vegetation and soils in AVIRIS Data. *Remote Sensing of Environment*, *44*, 255−269.

Shepherd, P. (2005). *SPUNMIX algorithm, PCI Geomatica 9.1.* North York, Ontario: Earth Observations Lab, Institute for Space and Terrestrial Science.

Smith, M. O., Johnson, P. E., & Adams, J. B. (1985). Quantitative determination of mineral types from reflectance spectra using principal components analysis. In *Proc. Fifteenth Lunar Planetary Sci. Conf. Part 2. J. Geophys. Res.*, *90*. (pp. C797−C804).

Smith, M. O., Ustin, S. L., Adams, J. B., & Gillespie, A. R. (1990). Vegetation in deserts: I. A regional measure of abundance from multispectral images. *Remote Sensing of Environment*, *31*, 1−26.

Sohn, Y., Moran, E., & Gurri, F. (1999). Deforestation in north-central Yucatan (1985–1995): Mapping secondary succession of forest and agricultural land use in Sotuta using the cosine of the angle concept. *Photogrammetric Engineering and Remote Sensing*, *65*(8), 947−958.

Soil Landscapes of Canada Working Group. (2007). *Soil Landscapes of Canada v3.1.1: Agriculture and Agri-Food Canada.*

South, S., Qi, J., & Lusch, D. P. (2004). Optimal classification methods for mapping agricultural tillage practices. *Remote Sensing of Environment*, *91*, 90−97.

Staenz, K. (1992). A decade of imaging spectrometry in Canada. *Canadian Journal of Remote Sensing*, *18*(4), 187−197.

Thoma, D. P., Gupta, S. C., & Bauer, M. E. (2004). Evaluation of optical remote sensing models for crop residue cover assessment. *Journal of Soil and Water Conservation*, *59* (5), 224−233.

Tompkins, S., Mustard, J. F., Pieters, C. M., & Forsyth, D. W. (1997). Optimization of endmembers for spectral mixture analysis. *Remote Sensing of Environment*, *59*, 472−489.

van Deventer, A. P., Ward, A. D., Gowda, P. H., & Lyon, J. G. (1997). Using Thematic Mapper data to identify contrasting soil plains and tillage practices. *Photogrammetric Engineering and Remote Sensing*, *63*, 87−93.

Willmott, C. J. (1982). Some comments on the evaluation of model performance. *Bulletin American Meteorological Society*, *63*(11), 1309−1313.